NATIONAL ADVISORY COMMITTEE FOR AERONAUTICS

TECHNICAL NOTE 2116

LINEARIZED SUPERSONIC AXIALLY SYMMETRIC FLOW ABOUT OPEN-NOSED BODIES OBTAINED BY USE OF STREAM FUNCTION

By Franklin Moore

Lewis Flight Propulsion Laboratory
Cleveland, Ohio

Washington
June 1950

NATIONAL ADVISORY COMMITTEE FOR AERONAUTICS

TECHNICAL NOTE 2116

LINEARIZED SUPERSONIC AXIALLY SYMMETRIC FLOW ABOUT OPEN-NOSED BODIES OBTAINED BY USE OF STREAM FUNCTION

By Franklin Moore

SUMMARY

The use of Stokes' stream function for axially symmetric problems in linearized supersonic flow is discussed. The computation of streamlines away from the body is shown to be facilitated by solving the stream-function problem rather than the potential problem. Use is made of the stream function throughout this report.

Half-power supersonic source distributions along the axis of symmetry are shown to provide streamlines that, at finite distances from the axis, turn a sharp corner at the Mach cone and are regular downstream of the Mach cone. Distributions of this type are used to provide the following procedures for open-nosed bodies of revolution at zero lift:

1. A numerical method for the computation of pressures along the body: The method, for which a simple example is given, is especially easy to apply on the forward part of the body.

2. Linearized formulas for the variation of strength and angle of the attached bow shock wave as functions of radial distance from the axis.

INTRODUCTION

In the design of a supersonic aircraft, the aerodynamics of an open-nosed component (for example, a ram-jet-engine housing) must often be described. In the analytical treatment of this type of problem, the determination of the flow about slender, open-nosed bodies of revolution at zero yaw may frequently be of value.

A standard method for computing the external pressure distribution associated with this type of flow is the numerical procedure described in reference 1, wherein a supersonic source distribution on the axis of symmetry is used to distort the free stream in such a way that one of the resulting stream surfaces approximately represents the body surface. A source distribution automatically meets two requirements of the problem:

1. The flow produced satisfies the linearized equations of motion of a compressible fluid.

2. Flow disturbances are limited to the region bounded by the outer surface of the body and the leading Mach wave proceeding outward and downstream from the lip, provided the source distribution is considered zero upstream of the apex of the Mach cone of which the leading Mach wave is a frustum.

A particular source distribution must be selected to provide a stream surface coincident with the body, to the first approximation in body slope. In the case of slender pointed bodies of revolution (reference 2), a simple relation exists between the source strength distribution and the slope of the body to be represented. The existence of this relation is due to the nearness of the body surface to the axis; the streamline slope at a point near the axis is a consequence only of the local value of the source-distribution function, to the first approximation.

When the body has an open nose, no such simplification may be considered to apply to its forward portion. The source distribution is then determined by an integral equation, which must be numerically solved, inasmuch as no closed solution seems available.

If the boundary condition on streamline slope at the body surface is applied on a mean cylinder, this integral equation may, in principle, be solved by operational methods, yielding solutions equivalent to those obtained for "quasi-cylindrical ducts" by Lighthill, whose work is summarized and extended in reference 3. The solutions appearing in reference 3 are given in integral form, and must be evaluated by numerical quadrature at each point where the pressure is to be determined. The accuracy of these results will suffer, in certain cases, from the application of boundary conditions at a mean cylinder.

A form for the source distribution is assumed in reference 1 (and in the present report) and the undetermined parameters are then selected in such a way that boundary conditions are satisfied with adequate accuracy. The form assumed in reference 1 is trapezoidal; that is, has a step-wise constant slope. The number of steps and their spacing is determined by the accuracy desired, and the slope of the distribution function between stations is determined by the shape of the body to be represented.

In selecting a form of solution wherein only certain parameters are available for variation, it is desirable to anticipate, insofar as possible, the features of the "exact" solution. On this basis, the trapezoidal distribution appears to have a certain disadvantage: namely, when approaching the intersections of the body surface with the Mach cones emanating from the points on the axis where the source-distribution slope is discontinuous, the streamline curvature tends toward infinity, whereas the streamline slope remains finite and continuous and, in fact, vanishes at the leading Mach wave. Verification of this statement is subsequently provided. This singular behavior of the streamline chosen to represent the body means that a large number of stations is required in regions of rapidly varying body slope, for example, near the lip of an open-nosed body. In particular, adequate evaluation of the local effect of discontinuous body slopes required a relatively dense local concentration of integration stations. An analysis of the linearized supersonic flow over the forward part of such bodies was made at the NACA Lewis laboratory and is presented herein.

A family of solutions is developed for axially symmetric open-nosed bodies at zero yaw, which may be combined to provide either smooth or polygonal streamlines, as desired, and whose parameters can conveniently be selected in order best to represent the forward part of a given body. In particular, solutions are sought that can be smoothly matched to the body in the same manner as a polynomial could be. The supersonic nature of the flow allows the superposition of smooth solutions in such a way as to provide streamline corners.

In brief, bodies encountered in practice will be smooth between and approaching corners. Solutions whose streamlines exhibit regular behavior near a leading Mach wave, but which may have corners precisely at the Mach wave, could therefore be matched to the forward portion of a given body with a minimum of "forcing" and hence a minimum of computational labor.

Use is made in this analysis of Stokes' stream function because solutions in terms of a stream function can readily be solved for streamlines, which may directly be compared with the given body contour. The stream function for linearized axially symmetric supersonic flow was used by Ferrari (reference 4), who developed the differential equation and solved it for pointed bodies of revolution by a Fourier integral method. In the analysis that follows, the use of the linearized stream function is discussed in somewhat more detail than appears in reference 4. In the interest of continuity, certain of Ferrari's results are rederived. The stream function is, of course, not essential to the analysis; equivalent results could be obtained by using the velocity potential.

SYMBOLS

The following symbols are used in this report:

C_p	pressure coefficient, $\dfrac{p-p_\infty}{\frac{1}{2}\rho_\infty u_\infty^2}$
E	complete elliptic integral of second kind
$f(x)$	local strength of supersonic source distribution
g, g_T, g_∞	dimensionless functions corresponding to Ψ, Ψ_T, and Ψ_∞, respectively
$H_n(\eta)$	flow function
K	complete elliptic integral of first kind
k_n	constant
M	Mach number
N	number of terms in terminated series
p	static pressure
$Q_n(\eta)$	flow function
R	radial coordinate of lip of open-nosed body
r	radial coordinate measured from, and normal to, axis of symmetry
r_E	radial coordinate with which given streamline enters leading Mach cone
s	dimensionless radial coordinate

$T_n(\eta)$	flow function
t	dimensionless axial coordinate
u	axial perturbation velocity
u_T	total axial-velocity component
u_∞	velocity of free stream
v	radial perturbation velocity
v_T	total radial-velocity component
x	axial coordinate measured in direction of axis of symmetry, origin at apex of leading Mach cone
y	variable of integration
α	initial body slope
β	cotangent of Mach angle of free stream, $\sqrt{M_\infty^{\ 2}-1}$
γ	ratio of specific heats
δ	small quantity depending on body shape, r_B-R
$\epsilon(t)$	body fineness parameter, s_B-1
η	ratio of s to t
θ, θ_D	angle between bow shock wave and axis of symmetry; θ_D refers to dimensionless coordinates
μ	measure of distance from lip, $x-\beta r_B$
ν	measure of distance from lip, $1-\eta$
ξ	variable of integration
ρ	density
$\sigma(\eta)$	argument of certain elliptic integrals
τ	variable of integration

φ variable of integration

$\Psi(x,r)$ perturbation stream function

$\Psi_T(x,r)$ Stokes' stream function for supersonic axially symmetric flow

Ψ_∞ free-stream value of stream function

Subscripts:

0 stagnation value

∞ free-stream value

B value on body

i index identifying point on body

The prime denotes ordinary differentiation.

ANALYSIS

Stokes' Stream Function for Linearized Supersonic Axially Symmetric Flow

Stokes' stream function may be defined in the following manner (reference 5, par. 94):

$$\left.\begin{aligned} u_T &\equiv \frac{\rho_\infty}{\rho}\frac{1}{r}\frac{\partial \Psi_T}{\partial r}(x,r) \\ v_T &\equiv -\frac{\rho_\infty}{\rho}\frac{1}{r}\frac{\partial \Psi_T}{\partial x}(x,r) \end{aligned}\right\} \qquad (1)$$

thus identically satisfying the exact equation of continuity (restricted to steady flow in this compressible case), which may be written

$$\frac{\partial}{\partial x}(\rho u_T) + \frac{1}{r}\frac{\partial}{\partial r}(r\rho v_T) = 0$$

By comparison with the treatment of the incompressible case in reference 5, it is clear that, here also, $d\Psi_T$ is an exact differential and represents the mass flux across a line element. Thus, a surface in space on which Ψ_T is constant is a stream surface of the flow.

In accordance with the assumptions of linearized theory,

$$\left.\begin{aligned} u_T &\equiv u_\infty + u \\ v_T &\equiv v \\ \Psi_T &\equiv \Psi_\infty + \Psi \end{aligned}\right\} \tag{2}$$

where $u,v \ll u_\infty$, and $\Psi \ll \Psi_\infty$. The introduction of these assumptions into the isentropic gas law

$$\left(\frac{\rho}{\rho_\infty}\right)^\gamma = \frac{p}{p_\infty}$$

and the energy equation, written in the form

$$\frac{p}{\rho} = \frac{p_0}{\rho_0} - \frac{\gamma-1}{2\gamma}\left(u_T^2+v_T^2\right)$$

yields the approximate relation

$$\frac{\rho_\infty}{\rho} \approx 1 + M_\infty^2 \frac{u}{u_\infty} \tag{3}$$

Substituting equations (2) and (3) into definitions (1) and collecting terms of like order yields

$$u_\infty = \frac{1}{r}\frac{\partial \Psi_\infty}{\partial r} \quad \text{or} \quad \Psi_\infty \equiv \frac{1}{2} u_\infty r^2 \tag{4}$$

$$u = -\frac{1}{\beta^2 r}\frac{\partial \Psi}{\partial r} \tag{5}$$

$$v = -\frac{1}{r}\frac{\partial \Psi}{\partial x} \tag{6}$$

Differential equation and boundary conditions. - Substitution of equations (5) and (6) into the irrotationality condition

$$\frac{\partial u}{\partial r} - \frac{\partial v}{\partial x} = 0$$

gives the following differential equation:

$$\beta^2 \frac{\partial^2 \Psi}{\partial x^2} - r \frac{\partial}{\partial r}\left(\frac{1}{r}\frac{\partial \Psi}{\partial r}\right) = 0 \tag{7}$$

The flow over a given slender obstacle is obtained by solving differential equation (7), subject to the following boundary conditions:

1. As in the case of the velocity potential, either a boundary condition at the bow Mach wave must be introduced or disturbances must be required to propagate only within downstream Mach cones, which is accomplished by use of the "supersonic source." In order that streamlines be everywhere continuous, the perturbation stream function Ψ must be continuous across the leading Mach wave (and hence must vanish as this Mach wave is approached from downstream). This fact is obvious when equations (5) and (6) are considered to be integrated for Ψ, the path of integration crossing the Mach cone.

2. On the body the boundary condition is that $\Psi_T = \frac{1}{2} u_\infty R^2$, where R is the radial distance of the leading edge from the axis of symmetry. Then,

$$\Psi\left(x, r_B(x)\right) = \frac{1}{2} u_\infty \left[R^2 - r_B{}^2(x)\right] \tag{8}$$

where $r_B(x)$ defines the body.

These boundary conditions, together with equation (7), provide a boundary-value problem of the first kind.

Stream function for supersonic source. - The function $-x/\sqrt{x^2-\beta^2 r^2}$ satisfies differential equation (7). This function is the stream function for the well-known supersonic source. A distribution of such sources along the x-axis yields

$$\left.\begin{aligned}\Psi &= -\int_0^{x-\beta r} \frac{f(\xi)(x-\xi)d\xi}{\sqrt{(x-\xi)^2-\beta^2 r^2}} \\ &= -\int_0^{x-\beta r} f'(\xi)\sqrt{(x-\xi)^2-\beta^2 r^2}\, d\xi \\ f(0) &= 0\end{aligned}\right\} \tag{9}$$

Substitution of equation (9) into equations (5) and (6) provides expressions for u and v identical to those provided by the distribution of source potentials (reference 2). Substitution of equation (9) into the boundary condition given by equation (8) provides an integral equation for $f(x)$. If a slender pointed body is under consideration, this integral equation (in which R is set equal to zero) may be differentiated with respect to x and then, provided $r_B(x)$ is vanishingly small, may be solved to yield the relation

$$\left.\begin{aligned}f(x) &= \frac{1}{2} u_\infty \frac{d}{dx}\left[r_B{}^2(x)\right]; \quad (x>0) \\ &= 0; \quad (x<0)\end{aligned}\right\} \tag{10}$$

where the origin of coordinates is placed at the nose of the body. This relation was first used by von Kármán (reference 2).

Example: right circular cone, at zero yaw, semivertex angle $\tan^{-1}\alpha$. - By use of the method of sources, equations (9) and (10) may be combined to yield the stream function for this flow. Alternatively, the solution may be obtained by direct integration of the differential equation, as follows: The solution may be written in the form $\Psi = r^2 h(\eta)$, where the origin is taken at the nose and $\eta \equiv \beta r/x$. This form for Ψ is chosen in order to insure that the flow will be "conical." Substitution in equation (7) yields an ordinary differential equation for $h(\eta)$. This equation may be solved to yield

$$\Psi = r^2\left[C_1\left(\frac{1}{\eta^2}\sqrt{1-\eta^2} - \cosh^{-1}\frac{1}{\eta}\right) + C_2\right]$$

where C_1 and C_2 are constants of integration to be determined from the boundary conditions. Inasmuch as the perturbation stream function must vanish on the bow wave $(\eta = 1)$, C_2 must be zero. The boundary condition given by equation (8) provides that

$$C_1 = -\frac{1}{2} u_\infty \left(\frac{1}{\beta^2\alpha^2}\sqrt{1-\beta^2\alpha^2} - \cosh^{-1}\frac{1}{\beta\alpha}\right)^{-1} \tag{11}$$

$$\approx -\frac{1}{2} u_\infty \beta^2\alpha^2$$

Therefore

$$\Psi = -\frac{1}{2} u_\infty \beta^2\alpha^2 r^2 \left(\frac{1}{\eta^2}\sqrt{1-\eta^2} - \cosh^{-1}\frac{1}{\eta}\right)$$

An identical result can be obtained by use of the source-distribution technique.

An interesting feature of the solution is noted:

The exact formulation of boundary conditions yields the value of C_1 given by equation (11). The axial perturbation velocity u may be obtained from the stream function as follows:

$$u = -\frac{u_\infty}{\beta^2}\left(\frac{1}{\beta^2\alpha^2}\sqrt{1-\beta^2\alpha^2} - \cosh^{-1}\frac{1}{\beta\alpha}\right)^{-1} \cosh^{-1}\frac{1}{\eta}$$

$$\approx -u_\infty\alpha^2 \cosh^{-1}\frac{1}{\eta}$$

The corresponding potential problem may be solved in a similar manner, in which case the use of exact boundary conditions provides that

$$u = -\frac{u_\infty}{\beta^2}\left(\frac{1}{\beta^2\alpha^2}\sqrt{1-\beta^2\alpha^2} + \frac{1}{\beta^2}\cosh^{-1}\frac{1}{\beta\alpha}\right)^{-1} \cosh^{-1}\frac{1}{\eta}$$

$$\approx -u_\infty\alpha^2 \cosh^{-1}\frac{1}{\eta}$$

Although the foregoing linearized results are identical, the exact solutions differ, thus emphasizing the incorrectness, in general, of using exact boundary conditions in the small-perturbation theory.

Use of stream function. - The use of the stream function has the primary advantage of providing a ready means of computing streamlines away from the body; for example, in the design of a tunnel-wall insert to eliminate wall interference. Equations (2) and (4), and the assumption that the stream function is continuous across the leading Mach cone, may be used to yield the following equation of a streamline:

$$\Psi_T = \frac{1}{2} u_\infty r_E^{\,2}$$

or

$$\frac{1}{2} u_\infty r^2 + \Psi = \frac{1}{2} u_\infty r_E^{\,2}$$

where the streamline is identified by the radial coordinate r_E with which it enters the Mach cone. For example, the following equation is obtained for a streamline of the cone flow treated in the preceding section:

$$\left(\frac{r_E}{r}\right)^2 = 1-\beta^2\alpha^2\left(\frac{1}{\eta^2}\sqrt{1-\eta^2} - \cosh^{-1}\frac{1}{\eta}\right)$$

If, in the course of calculations, it is necessary to find the family of streamlines associated with flow over a slender axially symmetric body at zero yaw, it would be simpler to formulate and to solve the problem in terms of the stream function.

A method of linearized characteristics based on equation (7) should yield the streamline family very quickly. Velocities could then be computed by forward differences.

Treatment of Open-Nosed Bodies of Revolution

An alternative numerical technique for open-nosed bodies, based on the use of the stream function produced by a source distribution, is developed in the following analysis:

The family of source distributions that gives polynomial streamline slopes near the lip of the body is sought. An illustrative open-nosed body is shown in figure 1. The definition

$$r_B(x) \equiv R + \delta(x)$$

where $\delta << R$,

is introduced into equation (8), yielding the approximate relation

$$\Psi(x, r_B(x)) \approx -u_\infty R\delta(x) \tag{12}$$

Equating expressions (9) and (12) yields

$$u_\infty R\delta(x) = \int_0^{x-\beta r_B} (x-\xi)\ f(\xi)\ \left[(x-\xi)^2 - \beta^2 r_B{}^2\right]^{-1/2} d\xi \tag{13}$$

Equation (13) may be expressed in terms of the quantity $\mu \equiv x-\beta r_B$, which is taken to be very small (thus restricting consideration to the vicinity of the lip). The following approximate equation results:

$$u_\infty \sqrt{\frac{2R}{\beta}}\ \delta(\mu) \approx \int_0^\mu \frac{f(\xi)d\xi}{\sqrt{\mu-\xi}}$$

This is Abel's integral equation, the solution of which is, according to reference 6 (par. 11.8):

$$f(x) = \frac{u_\infty}{\pi}\sqrt{\frac{2R}{\beta}}\ \frac{d}{dx}\int_0^x \frac{\delta(\xi)d\xi}{\sqrt{x-\xi}} \tag{14}$$

whence,

1. If $\delta(\mu) \propto \mu$, then equation (14) provides that $f(x) \propto x^{1/2}$.

2. If $\delta(\mu) \propto \mu^2$, then $f(x) \propto x^{3/2}$.

3. If $\delta(\mu) \propto \mu^3$, then $f(x) \propto x^{5/2}$, and so forth.

A similar analysis will show that if $f(x) \propto x$ (as in the method of reference 1), then $\delta(\mu) \propto \mu^{3/2}$. Thus, as stated in the INTRODUCTION, the open-nosed body associated with a linear source distribution has at the lip $(\mu = 0)$ a vanishing slope and an infinite curvature.

In view of the foregoing results, a sequence of solutions for Ψ are sought, each solution (Ψ_n) corresponding to a source distribution on the axis of symmetry, of the form $x^{n-1/2}$, where n equals 1, 2, 3, ...

These solutions can be combined to represent a given body, with the assurance that this representation of the body will be regular (that is, will have a Taylor expansion) near the lip.

The following dimensionless quantities are defined:

$$\left.\begin{aligned} & t \equiv \frac{x}{R\beta} \qquad s \equiv \frac{r}{R} \qquad \eta \equiv \frac{s}{t} \\ & g_T = g_\infty + g, \quad \text{where} \quad g \equiv \frac{\Psi}{u_\infty R^2}, \quad \text{and so forth} \end{aligned}\right\} \tag{15}$$

By comparison of these definitions with equations (4), (5), and (7),

$$g_T = \frac{1}{2} s^2 + g \tag{16}$$

$$\frac{u}{u_\infty} = -\frac{1}{\beta^2}\frac{1}{s}\frac{\partial g}{\partial s}$$

$$\frac{\partial^2 g}{\partial t^2} - s\frac{\partial}{\partial s}\left(\frac{1}{s}\frac{\partial g}{\partial s}\right) = 0$$

Using the usual linearized form for the pressure coefficient yields

$$C_p = -2\frac{u}{u_\infty} = \frac{2}{\beta^2}\frac{1}{s}\frac{\partial g}{\partial s} \tag{17}$$

Near the lip of an open-nosed body, the two-dimensional character of the flow insures the validity and the adequacy of equation (17). Far downstream of the lip, provided there are no further streamline corners, the flow will approach that for the corresponding pointed-nose body of revolution. Higher order terms appearing in Bernoulli's equation would then be of sufficient order of magnitude for inclusion in the formula for pressure coefficient, although a strict mathematical basis for their inclusion would be lacking. Because this report places emphasis on the forward portion of the body, additional discussion of this question would not be pertinent.

In the notation of equation (15), a sequence of stream functions g_n are to be obtained, each member of the sequence to correspond to a certain axial source-distribution function f_n. Thus, when definitions (15) are substituted into equation (9) and the variable of integration is suitably redefined, the following expression (aside from a constant) is obtained:

$$g_n = -\int_0^{t-s} f_n'(\tau)\left[(t-\tau)^2-s^2\right]^{1/2} d\tau \tag{18}$$

In accordance with the previous discussion, f_n is chosen to be

$$f_n(t) \equiv k_n t^{n-1/2} \tag{19}$$

where n is an integer, and k_n is an undetermined constant. Substitution of equation (19) into equation (18) and integration according to the method set forth in appendix A provide the following results for g_n and, by superposition, a terminating series of N terms for g:

$$\left.\begin{aligned} g_n &= k_n t^{n+1/2} H_n(\eta) \\ g &= \sum_1^N k_n t^{n+1/2} H_n(\eta) \end{aligned}\right\} \tag{20}$$

By use of equation (17) $\beta^2 C_{p_n}$ may be expressed in terms of g_n:

$$\left.\begin{aligned} \beta^2 C_{p_n} &= k_n t^{n-3/2} T_n(\eta) \\ \beta^2 C_p &= \sum_1^N k_n t^{n-3/2} T_n(\eta) \end{aligned}\right\} \tag{21}$$

where

$$
\left.
\begin{aligned}
H_1(\eta) &\equiv -2\sqrt{1+\eta}\,\frac{1}{3}\left[-\eta K(\sigma) + E(\sigma)\right] \\
H_n(\eta) &\equiv \frac{2n-1}{2n+1}\left[2\eta^2\sqrt{1+\eta}\,(K-E) + H_{n-1} + \eta^2(H_{n-2}\ H_{n-3} + \ldots + H_1)\right] \\
&\qquad\qquad\qquad n > 1
\end{aligned}
\right\} \tag{22}
$$

$$
\left.
\begin{aligned}
T_1(\eta) &\equiv 2\,\frac{1}{\sqrt{1+\eta}}\,K(\sigma) \\
T_n(\eta) &\equiv \frac{2n-1}{2n+1}\left\{\frac{2}{\eta}\sqrt{1+\eta}\left[\frac{\eta}{1+\eta}\,(4+5\eta)K-5\eta E\right] + \right. \\
&\qquad T_{n-1} + \eta^2(T_{n-2}+T_{n-3}+ \ldots +T_1) + \\
&\qquad \left. 4(H_{n-2}+H_{n-3}+ \ldots +H_1)\right\}, \qquad n > 1
\end{aligned}
\right\} \tag{23}
$$

and

$$
\left.
\begin{aligned}
K(\sigma) &\equiv \int_0^{\pi/2} d\varphi\,(1-\sigma^2\sin^2\varphi)^{-1/2} \\
E(\sigma) &\equiv \int_0^{\pi/2} d\varphi\,(1-\sigma^2\sin^2\varphi)^{1/2} \\
\sigma &\equiv \sqrt{\frac{1-\eta}{1+\eta}}
\end{aligned}
\right\} \tag{24}
$$

(The symbols K and E are complete elliptic integrals of the first and second kinds, respectively.) The $H_n(\eta)$ and $T_n(\eta)$ are tabulated in table I, for $n = 1, 2, 3, 4$, and 5.

The equation for determining the constants k_n is developed as follows: On the body, the boundary condition given by equation (8) requires that

$$g = \frac{1}{2}\left(1 - s_B{}^2\right)$$

Thus, equation (20) provides that

$$\epsilon\Big(t_B(\eta)\Big)\left[1 + \frac{1}{2}\,\epsilon\Big(t_B(\eta)\Big)\right] = -g\Big(t_B(\eta),\eta\Big) = -\sum_1^N k_n t_B(\eta)^{n+\frac{1}{2}} H_n(\eta) \tag{25}$$

where

$$s_B \equiv 1 + \epsilon(t)$$

Because k_1 corresponds to $f(t) \propto t^{1/2}$ and $t^{1/2}$ is the only distribution function providing a nonvanishing streamline slope at the lip, k_1 is determined solely by the initial body slope. Near $\eta = 1$, let $\eta \equiv 1 - \nu$, where $\nu << 1$, and thus $t_B \approx 1 + \nu$. Equation (25) then becomes

$$\epsilon \approx -k_1 H_1\ (1 - \nu) \tag{26}$$

From equation (24),

$$K\left(\sqrt{\frac{\nu}{2}}\right) \approx \frac{\pi}{2} + \frac{\nu}{4}\int_0^{\pi/2} \sin^2\varphi\ d\varphi$$

$$E\left(\sqrt{\frac{\nu}{2}}\right) \approx \frac{\pi}{2} - \frac{\nu}{4}\int_0^{\pi/2} \sin^2\varphi\ d\varphi$$

Thus,

$$-\eta K + E \approx \frac{3}{8}\pi\nu$$

or

$$H_1(1-\nu) \approx -\frac{\pi}{2\sqrt{2}}\,\nu$$

By use of the fact that $t \approx 1 + \nu$ on the body, equation (26) may be differentiated to provide

$$k_1 = \frac{2\sqrt{2}}{\pi}\Big[\epsilon'(t)\Big]_{t=1}$$

$$\equiv \frac{2\sqrt{2}}{\pi}\epsilon'(1) \tag{27}$$

The remaining values of k_n are computed as follows:

1. Equation (25) is formulated at $N-1$ points on the body (exclusive of the lip, because all the H_n vanish for $\eta = 1$).

2. The resulting set of $N-1$ linear algebraic equations is solved for $k_2, k_3, \ldots, k_N$.

When the constant k_n has been determined, $\beta^2 C_p$ is computed directly from equation (21). A more detailed outline of numerical procedure will be subsequently presented.

Linearized treatment of attached bow shock. - The first approximation to the strength of the bow shock for an open-nosed body may easily be obtained from g_1 because, in the linear theory, characteristics of the same family never intersect, thus providing that the shock strength is a function only of the initial body slope. Defining the shock strength as $\Delta(\beta^2 C_p)$ across the shock yields

$$\Delta(\beta^2 C_p) = k_1 t^{-1/2} \lim_{\eta \to 1} T_1(\eta)$$

where η approaches 1 from below.

From equations (23) and (24),

$$\lim_{\eta \to 1} T_1(\eta) = \sqrt{2}\int_0^{\pi/2} d\varphi = \frac{\pi}{\sqrt{2}}$$

and applying equation (27),

$$\left.\begin{aligned} \Delta(\beta^2 C_p) &= 2\epsilon'(1)t_E^{-1/2} = 2\epsilon'(1)s_E^{-1/2} \\ \text{or} \qquad & \\ \Delta(C_p) &= \frac{2}{\beta}\,\delta'(\beta R)\left(\frac{r_E}{R}\right)^{-1/2} \end{aligned}\right\} \tag{28}$$

Equation (28) gives the linearized rule for the attenuation of the shock strength with increasing distance from the axis of symmetry. (Note that when $r_E/R = 1$, equation (28) gives the two-dimensional result.)

In view of the foregoing result, it should be possible to propose a formula for the shape of the bow wave. Such a formula should, of course, be checked against a solution by the method of characteristics in order to establish its value. At first it would seem that a first-order determination of the shape of the bow shock wave would be in conflict with one of the basic results of the first-order (linearized) theory, namely, that all shock and expansion waves appear to be located at Mach surfaces.

The exact oblique-shock-wave relations may, however, be used to show that a first-order flow deflection through a shock wave is associated with a first-order variation of shock position from that of the Mach surface. Hence, if formulas are available for the flow deflection and the pressure rise across the shock, both presumed accurate to first order, and if they are consistent (to the first order) with the requirements of the oblique-shock relations, these pressure and deflection functions may be used to determine, to the first order, the only remaining quantity involved in the shock relations, namely, the shock inclination.

1. In order to show that the pressure-rise and flow-deflection formulas stand in the proper relation, equation (28) is first modified to

$$\Delta\left(\frac{u}{u_\infty}\right) = -\frac{1}{\beta}\,\delta'(\beta R)\left(\frac{r_E}{R}\right)^{-1/2} \tag{29}$$

Equation (16) may be written as follows when equations (20) and (27) and a definition of s_E as the radial coordinate of the streamline entering the Mach surface are used:

$$\frac{1}{2}s_E^{\,2} = \frac{1}{2}s^2 + \frac{2\sqrt{2}}{\pi}\epsilon'(1)t^{3/2}H_1(\eta)$$

(Note that inasmuch as this is the equation of a streamline, s is to be considered a function of t.)

The derivative of the preceding equation may be evaluated at $\eta = 1$ to provide the flow deflection through the shock. The following result is obtained:

$$\left.\begin{aligned} \left(\frac{\partial s}{\partial t}\right)_{\eta=1} &= \epsilon'(1)s_E^{-1/2} \\ &\text{or} \\ \left(\frac{\partial r}{\partial x}\right)_{\eta=1} &= \delta'(\beta R)\left(\frac{r_E}{R}\right)^{-1/2} \end{aligned}\right\} \tag{30}$$

This result was previously obtained in reference 3, wherein an entirely different approach was used. Adding equations (29) and (30) yields

$$\beta\,\Delta\left(\frac{u}{u_\infty}\right) = -\left(\frac{\partial r}{\partial x}\right)_{\eta=1} \tag{31}$$

Equation (31) must now be shown to be consistent with the oblique-shock relations. The angle between the shock wave and the axis of symmetry, in the original (x,r) coordinates, is defined to be θ. This definition may be introduced into equation 4.22 of reference 7, which then may be written as

$$\tan\theta = -\frac{\Delta u}{v} = -\frac{\Delta u}{(u_\infty+\Delta u)\left(\frac{\partial r}{\partial x}\right)_{\eta=1}}$$

or, inasmuch as $\tan\theta \approx 1/\beta$,

$$\frac{1}{\beta} \approx -\frac{\Delta\frac{u}{u_\infty}}{\left(\frac{\partial r}{\partial x}\right)_{\eta=1}}$$

which clearly reduces to the first-order relation given in equation (31).

2. The shock-wave inclination may now be determined. Equation 4.29 of reference 7 may be written as

$$1 + \frac{\gamma}{2} M_\infty^2 \Delta(C_p) = \frac{2\gamma}{\gamma+1} M_\infty^2 \sin^2 \theta - \frac{\gamma-1}{\gamma+1}$$

or

$$\tan^2 \theta = \frac{1}{\beta^2} \frac{1 + \frac{\gamma+1}{4} M_\infty^2 \Delta(C_p)}{1 - \frac{\gamma+1}{4} \frac{M_\infty^2}{\beta^2} \Delta(C_p)}$$

From equation (28),

$$\Delta(C_p) = \frac{2}{\beta} \delta'(\beta R)\left(\frac{r_E}{R}\right)^{-1/2}$$

and thus, because $\Delta(C_p)$ is a small quantity,

$$\tan \theta \approx \frac{1}{\beta} + \frac{\gamma+1}{8} \frac{M_\infty^4}{\beta^3} \Delta(C_p)$$

or

$$\tan \theta \approx \frac{1}{\beta} + \frac{\gamma+1}{4} \frac{M_\infty^4}{\beta^4} \delta'(\beta R)\left(\frac{r_E}{R}\right)^{-1/2} \tag{32}$$

If θ_D is defined at the shock inclination (fig. 1) in the coordinates introduced in equations (15), equation (32) becomes

$$\tan \theta_D \approx 1 + \frac{\gamma+1}{4} \frac{M_\infty^4}{\beta^4} \epsilon'(1) s_E^{-1/2} \tag{33}$$

Equation (33) is exact at an infinite distance from the body. The error at the lip of the body should indicate the magnitude of error at finite distances from the surface. For a free-stream Mach number of 1.50 in air $(\gamma = 1.4)$ and an initial body slope of 5 percent, the exact oblique-shock relations yield a value of $\tan\theta = 1$ at the lip; whereas equation (33) gives $\tan\theta = 0.988$. These results are to be compared with a Mach angle equal to $\tan^{-1} 0.894$. At the lip, equation (33) is therefore in error by about 1 percent in predicting the shock angle and by about 12 percent in predicting the difference between shock and Mach angles.

METHOD FOR PRESSURE CALCULATION AND EXAMPLE

The functions T_n and H_n, appearing in equations (21) and (25), respectively, are tabulated in table I. The reciprocal sequence of η provides approximately equal intervals of $t_B(\eta)$ for a slender body, thus making it unnecessary to perform interpolations. The following numerical procedure is recommended:

1. Select the number $(N-1)$ and location (η_i) of the points (exclusive of the lip) through which the streamlines will be required to pass. Define these points by values of η for which the functions in table I are given.

2. Compute $t_B(\eta_i)$ from the equation of the body and tabulate $t_B(\eta_i)^{-1/2}$, $t_B(\eta_i)^{1/2}$, . . . , $t_B(\eta_i)^{N+1/2}$.

3. Compute k_1 from the initial slope of the body, using equation (27).

4. Formulate equation (25) at the $N-1$ "matching points," and solve the $N-1$ simultaneous equations for $k_2, k_3, \ldots, k_N$.

5. Use the k_n thus determined to compute $\beta^2 C_p$ at any desired location, using equation (21).

This procedure has been carried out for a truncated cone of slope $\epsilon'(1) = 0.0523$, matching streamlines at $\eta = 1/2$, $1/3$, and $1/4$, and at $\eta = 1/2$ and $1/3$. The results appear in figure 2. Comparison is made with the result obtained by the method of reference 1 for a truncated cone of the same slope, using approximately eight integration points in the range of t shown (reference 8). An additional curve shown in figure 2 was obtained by applying the boundary condition on streamline slope at $\eta = 1/2$, $1/3$, and $1/4$ on the body, and computing C_p, as was previously done. Appendix B contains the pertinent analysis and procedure, which gives rise to the function $Q_n(\eta)$ plotted in table I.

In order to determine the accuracy attained by using a certain set of matching points, equation (25) may easily be inverted and solved for ϵ at intermediate points. These values of ϵ should, of course, fall on the surface of the given body, with an error of the order of ϵ^2. This inversion may be carried out with sufficient accuracy by assuming that $t_B(\eta)$ at the intermediate points is given by the equation of the body.

As a guide to the selection of matching points, the following generalizations are offered:

1. The farther downstream the computations are to be extended, the denser must be the matching-point distribution. (In the method of reference 1, the density of integration stations must be greatest near the lip.) This question of convergence will be subsequently discussed.

2. Very few points are needed near the lip.

3. Pressure values cannot be computed with adequate accuracy at points downstream of the last matching point.

DISCUSSION OF METHOD FOR PRESSURE CALCULATION

The use of the half-power source distribution on the axis of symmetry provides a family of stream functions that are easily related to the forward portion of a given body. The component stream functions of equation (25), however, become infinite at $y = 0$ and, as computations are extended downstream, satisfactory convergence is obtained with increasing difficulty; that is, the matching-point density must be greater. Near the lip of an open-nosed body, the present method therefore converges rapidly; whereas the method of reference 1 converges slowly (the computations of reference 1 do not automatically provide the two-dimensional solution at the lip, but rather converge to that solution as more and more integration stations are used). Toward the aft portion of the body, the reverse is true.

Good agreement between the method proposed herein and the method of reference 1, on the forward portion of the body, is shown in figure 2. Farther downstream, the result begins to diverge from the proper one - for the reason previously mentioned. In order to extend the solution downstream, more matching points would have to be provided.

Of course, the stream function is not essential to the present technique, nor is it the cause of the downstream divergence of the method. For the case computed, the curve in figure 2 obtained by matching streamline slopes (as is customary in analysis based on the velocity potential) diverges from the proper result farther downstream than does the corresponding curve obtained by matching streamline locations.

CONCLUSIONS

Stokes' stream function for supersonic linearized flow may be used to advantage whenever it is desirable to deal directly with streamlines.

Use of half-power source distributions on the axis of symmetry gives a family of stream functions having streamlines regular near the lip of an open-nosed body of revolution. These streamlines, being regular, are easily matched to the forward portion of a given body.

First-order relations have been obtained for the attenuation of shock strength and flow deflection outward along the shock and for the corresponding shock-wave inclination. These results should be checked against experiment or the method of characteristics before being applied to practical problems. It is felt that these relations would probably conform rather well to physical fact, provided the entrance slope is small. These relations contain an error of the order of $[\delta'(\beta R)]^2$ at the lip of the body (where δ is a small quantity depending on the body shape, β is the cotangent of the Mach angle, and R is the radial coordinate of the lip of the body), and become exact as the radial coordinate r approaches infinity. It thus seems plausible that the error in the formulas for shock strength and inclination would be of second order over the entire shock front.

Lewis Flight Propulsion Laboratory,
National Advisory Committee for Aeronautics,
Cleveland, Ohio, December 5, 1949.

APPENDIX A

METHOD OF EVALUATING g_n

Equation (18) may be written, after the substitution of equation (19), as

$$g_n = -k_n\left(n-\frac{1}{2}\right)\int_0^{t-s}\left[(t-\tau)^2-s^2\right]^{1/2}\tau^{n-3/2}\,d\tau \tag{A1}$$

The following change of variable of integration is introduced:

$$y \equiv \left(\frac{1}{1-\eta}\,\frac{\tau}{t}\right)^{1/2}$$

This substitution yields elliptic integrals in Legendre's canonical forms. From reference 6 (par. 22.72),

$$\int_0^1 dy\left[(1-y^2)(1-\sigma^2y^2)\right]^{-1/2} = K(\sigma) \tag{A2}$$

$$\int_0^1 y^2dy\left[(1-y^2)(1-\sigma^2y^2)\right]^{1/2} = \frac{1}{\sigma^2}\left[K(\sigma)-E(\sigma)\right] \tag{A3}$$

differentiating and integrating the expression

$$y^{2n-1}\left[(1-y^2)(1-\sigma^2y^2)\right]^{1/2}$$

yields the following recursion equation:

$$(2n-1)\int_0^1 y^{2n-2}dy\left[(1-y^2)(1-\sigma^2 y^2)\right]^{-1/2} - 2n(1+\sigma^2)\int_0^1 y^{2n}dy\left[.\ .\ .\right]^{-1/2} +$$

$$(2n-1)\sigma^2\int_0^1 y^{2n+2}dy\left[.\ .\ .\right]^{-1/2} = 0 \qquad \text{(A4)}$$

Equations (A2), (A3), and (A4) permit equation (A1) to be expressed in terms of $K(\sigma)$ and $E(\sigma)$.

In computing velocities, use is found for the following equations (reference 6, par. 22.736):

$$\frac{dE(\sigma)}{d\sigma^2} = \frac{1}{2\sigma^2}\left[E(\sigma)-K(\sigma)\right]$$

$$\frac{dK(\sigma)}{d\sigma^2} = \frac{1}{2\sigma^2}\left[\frac{1}{1-\sigma^2}E(\sigma)-K(\sigma)\right]$$

APPENDIX B

BOUNDARY CONDITION ON STREAMLINE SLOPE

In the numerical method developed for the determination of pressure on an open-nosed body, a boundary condition (equation (8)) on the stream function has been applied. Alternatively, a boundary condition on streamline slope may be used as follows: The boundary condition is

$$\left(\frac{v}{u_\infty+u}\right)_B \approx \left(\frac{v}{u_\infty}\right) = \delta'(x)$$

which becomes, after definitions (5) and (6) are introduced,

$$-\frac{1}{s_B}\left(\frac{\partial g}{\partial t} - \frac{\eta}{t}\frac{\partial g}{\partial \eta}\right)_B = \epsilon'(t) \qquad \text{(B1)}$$

Equations (15), (17), and (21) enable $\frac{\partial g}{\partial \eta}$ to be expressed in terms of $T_n(\eta)$, and equation (20) provides a relation between $\frac{\partial g}{\partial t}$ and and $H_n(\eta)$. Thus, equation (B1) becomes

$$\epsilon'(t_B(\eta)) = \sum_1^N k_n\ t_B(\eta)^{n-3/2} Q_n(\eta) \qquad \text{(B2)}$$

where

$$Q_n(\eta) \equiv \frac{1}{2}\eta\ T_n(\eta) - \left(n+\frac{1}{2}\right)\frac{1}{\eta}H_n(\eta)$$

Values of the function $Q_n(\eta)$ may be found in table I.

The method for pressure calculation using the boundary condition on streamline slope is precisely the same as that previously described, with the exception that equation (B2) has the role heretofore played by equation (25).

REFERENCES

1. Brown, Clinton E., and Parker, Hermon M.: A Method for the Calculation of External Lift, Moment, and Pressure Drag of Slender Open-Nose Bodies of Revolution at Supersonic Speeds. NACA Rep. 808, 1945. (Formerly NACA ACR L5L29.)

2. de Kármán, Th.: The Problem of Resistance in Compressible Fluids. Quinto Convegno "Volta", Reale Accademia d'Italia (Roma), Sett. 30-Ott. 6, 1935, pp. 3-57.

3. Ward, G. N.: The Approximate External and Internal Flow past a Quasi-Cylindrical Tube Moving at Supersonic Speeds. Quarterly Jour. Mech. and Appl. Math., vol. 1, pt. 2, 1948, pp. 225-245.

4. Ferrari, C.: The Determination of the Projectile of Minimum Wave Resistance. R. T. P. Trans. No. 1180, British M.A.P.

5. Lamb, Horace: Hydrodynamics. Cambridge Univ. Press, 6th ed., 1932, pp. 125-126.

6. Whittaker, E. T., and Watson, G. N.: Modern Analysis. The Macmillan Co. (New York), 1943, pp. 229, 514-516, 521.

7. Liepmann, Hans Wolfgang, and Puckett, Allen E.: Introduction to Aerodynamics of a Compressible Fluid. John Wiley & Sons, Inc., 1947, pp. 52, 57.

8. Jack, John R.: Theoretical Wave Drags and Pressure Distributions for Axially Symmetric Open-Nose Bodies. NACA TN 2115, 1950.

TABLE I - FUNCTIONS USED FOR COMPUTING STREAMLINES AND PRESSURES

$1/\eta$	$-H_1$	$-H_2$	$-H_3$	$-H_4$	$-H_5$
1	0	0	0	0	-0
1.25	.20766	.03054	.00475	.00032	-.00080
1.5	.32871	.07922	.02042	.00392	-.00194
2	.46001	.16453	.06697	.02903	-.01318
3	.56426	.26112	.13912	.07914	-.04681
4	.60436	.30799	.18195	.11505	-.07560
5	.62480	.33451	.20873	.13987	-.09763
6	.63624	.35063	.22603	.15679	-.11344
7	.64346	.36132	.23797	.16893	-.12519
8	.64849	.36888	.24667	.17802	-.13426
9	.65204	.37437	.25311	.18487	-.14121
10	.65454	.37845	.25801	.19019	-.14669
12	.65764	.38390	.26475	.19770	-.15460
14	.65986	.38758	.26935	.20286	-.16011
16	.66114	.39001	.27246	.20642	-.16400
$1/\eta$	T_1	T_2	T_3	T_4	T_5
1	2.22171	0	0	0	0
1.25	2.41109	.73505	.18679	.04786	.01895
1.5	2.57167	1.32770	.56925	.24245	.12785
2	2.83099	2.22958	1.41591	.83058	.46526
3	3.21120	3.48473	2.98658	2.35334	1.77371
4	3.48788	4.37032	4.26209	3.81094	3.26231
5	3.70498	5.04664	5.28699	5.06011	4.62728
6	3.88312	5.59980	6.15194	6.15842	5.88378
7	4.03528	6.06782	6.89588	7.12501	7.01890
8	4.16621	6.46680	7.53546	7.96738	8.02372
9	4.28338	6.82305	8.11157	8.73563	8.95364
10	4.38734	7.13981	8.62701	9.42871	9.80062
12	4.56878	7.69240	9.53250	10.65814	11.32064
14	4.72204	8.15524	10.29267	11.69685	12.61471
16	4.85539	8.55928	10.95993	12.61379	13.76563
$1/\eta$	Q_1	Q_2	Q_3	Q_4	Q_5
1	1.11086	0	0	0	0
1.25	1.35380	.38946	.09550	.02094	.00208
1.5	1.59683	.73965	.29696	.10728	.02661
2	2.08778	1.38005	.82277	.46892	-.02866
3	3.07436	2.53920	1.95852	1.46061	-.47675
4	4.06215	3.62619	3.08006	2.54727	-1.25541
5	5.05650	4.68604	4.18148	3.65309	-2.22210
6	6.04978	5.72611	5.25930	4.74654	-3.25320
7	7.04457	6.75652	6.32284	5.83024	-4.31846
8	8.04227	7.78178	7.37773	6.90668	-5.40596
9	9.04050	8.80238	8.42361	7.97255	-6.49248
10	10.03747	9.81824	9.46170	9.02999	-7.57792
12	12.02788	11.83750	11.51667	11.11987	-9.73193
14	14.02571	13.85656	13.56575	13.19793	-11.87794
16	16.01909	15.86788	15.60026	15.25642	-14.00182

NACA

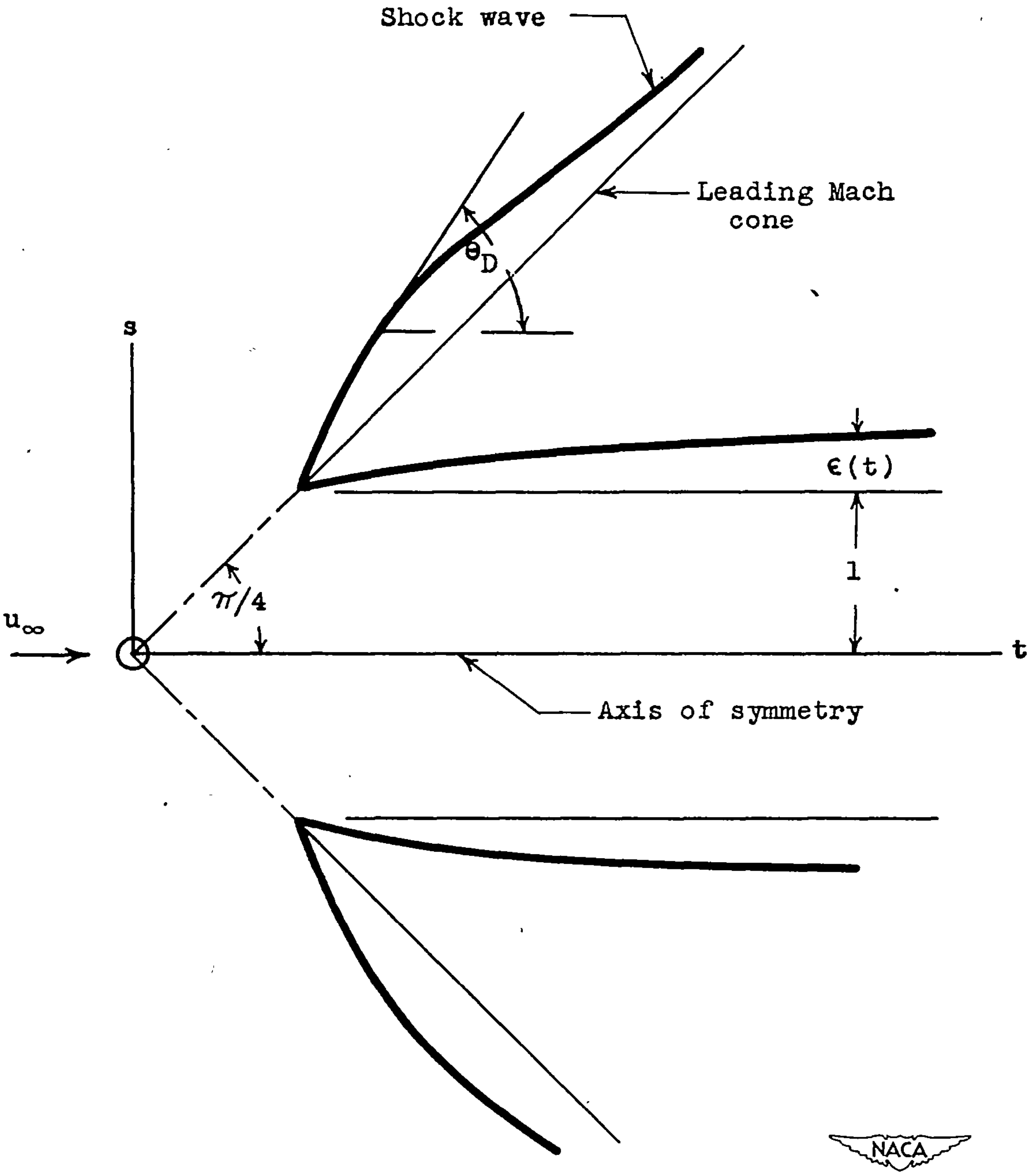

Figure 1. - Illustrative open-nosed body.

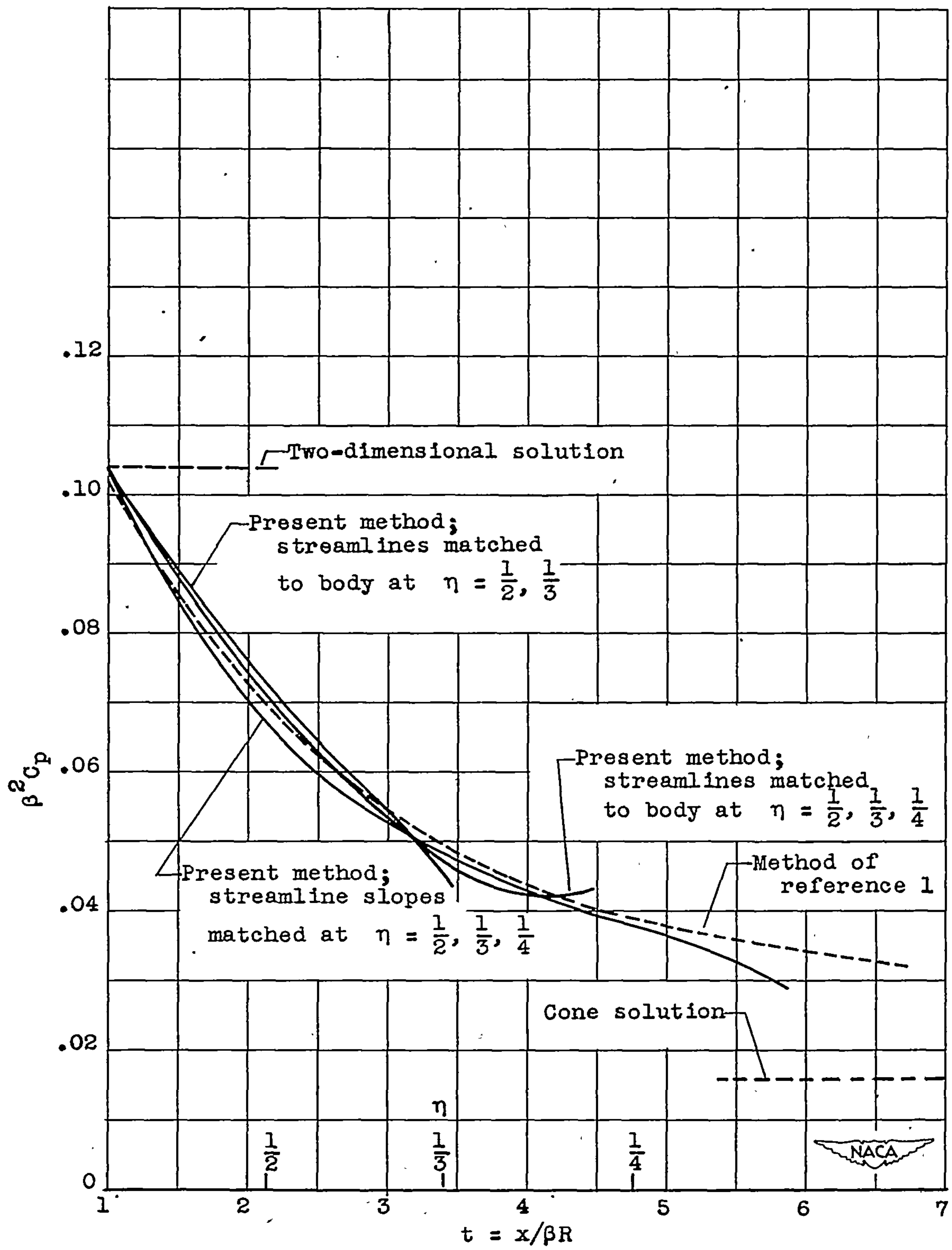

Figure 2. - Pressure on a truncated cone. $\epsilon'(1)$, 0.0523.

NACA-Langley - 6-19-50 - 1000